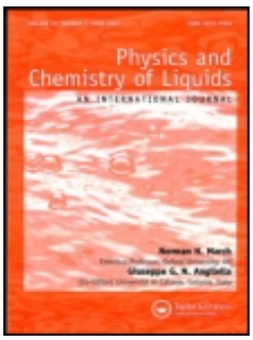

Physics and Chemistry of Liquids
An International Journal

ISSN: 0031-9104 (Print) 1029-0451 (Online) Journal homepage: http://www.tandfonline.com/loi/gpch20

Structure and dynamics of undercooled FeNi

W.C. Cui , C.X. Peng , L. Wang , Y. Qi & T. Fang

To cite this article: W.C. Cui , C.X. Peng , L. Wang , Y. Qi & T. Fang (2014) Structure and dynamics of undercooled FeNi, Physics and Chemistry of Liquids, 52:1, 88-99, DOI: 10.1080/00319104.2013.802209

To link to this article: http://dx.doi.org/10.1080/00319104.2013.802209

Published online: 04 Jun 2013.

Physics and Chemistry of Liquids, 2014
Vol. 52, No. 1, 88–99, http://dx.doi.org/10.1080/00319104.2013.802209

Structure and dynamics of undercooled FeNi

W.C. Cui, C.X. Peng, L. Wang*, Y. Qi and T. Fang

School of Mechanical & Electrical and Information Engineering, Shandong University at Weihai, Weihai, China, 264209

(*Received 22 March 2013; final version received 20 April 2013*)

Molecular dynamics simulation has been performed to explore the structural and dynamical properties of undercooled FeNi melt based on the embedded atom method (EAM), namely due to G. Bonny. The simulated partial pair correlation function (PPCF) and coordination number (CN) of liquid FeNi indicate that no stronger interaction of heterogenic atom pairs than those of the same atom pairs happen in melts. FeNi melt is close to an ideal mixing system without chemical short-range order (CSRO). The undercooled FeNi exhibits icosahedral short-range order (ISRO) that is reflected directly as a large number of 1551, 1541 bonded pairs as well as snapshot of icosahedron clusters. The mean squared displacement (MSD) and self diffusion coefficient of Fe and Ni is quite similar, which is consistent with the strong glass formation liquid of Ni36Zr64. Our work gives the detailed structure and dynamics information of undercooled FeNi melt.

Keywords: Icosahedral short-rang order; FeNi undercooled liquid; structure and dynamics relaxation; molecular dynamics simulation

1. Introduction

A good glass formation ability (GFA) of liquid alloys can be achieved when the liquid phase is stabilised by enhancing the local structure ordering in the near-neighbour region and by restraining the progress of the nucleation and growth of crystallites starting from the embryo in the liquid phase [1]. Over the past several decades, a series of empirical rules have been developed to help in the selection of alloys [2]. Liquids that stay stable to such a low temperature would therefore have slower diffusion in the undercooled liquid, thereby preventing crystal growth. Also, it has been found that bulk metallic glasses have densities close to their crystalline counterparts, which indicates that the packing of atoms in this amorphous structure is very efficient and energetically stable [3]. Short-range order in undercooled metallic liquids plays an essential role in glass formation in these systems. Many experiments using scattering and absorption techniques have been employed to study the short-range order of melts. Meanwhile, computer simulations have also been widely used to study the atomic structure evolution in liquid metallic alloys. As a result of these efforts, local cluster structures for some model binary systems have been demonstrated. It was originally proposed that icosahedral ordering in the liquid are efficiently packed and they are therefore energetically stable clusters that serve to stabilise the liquid by serving as an energetic barrier against nucleation [4]. These types of clusters are also known to lead to slow dynamics in the liquid [5]. Based on these ideas, it can be assumed

*Corresponding author. Email: wanglihxf@sdu.edu.cn

that a large fraction of icosahedra in the liquid state can allow for a metal to more easily prevent crystallisation.

The fragility of a liquid is a measure of how its viscosity changes as a function of temperature. The main concept behind tying this parameter to glass-forming ability is that liquids with a high viscosity have slow kinetics, which inhibits the growth of crystals [6]. A glass with a low fragility parameter slowly changes viscosity as temperature is increased past the glass-transition temperature [7]. Correct descriptions of the thermodynamic, dynamic and structural relaxation of glass-forming liquids within the temperatures at which the viscosity is much higher are still not really known, and this has been the focus of our current research. Since the first Fe-based amorphous Fe-P-C alloy was synthesised in 1967, Fe-based amorphous alloys have gained the most important position in the field of amorphous alloys. The search for Fe-based amorphous alloys with a wide undercooled liquid region is very important because the existence of the undercooled liquid region indicates the high thermal stability of the undercooled liquid against crystallisation, which implies the possibility of forming bulk amorphous alloys with good soft magnetic properties.

Compared with other glass-forming liquids, the structure of Fe-Ni liquid is much simple and close to dense random packing of spheres without the complex intramolecular effect. Therefore, it offers a good opportunity for understanding the universal mechanism of complex relations in undercooled liquids. This article provides a theoretical estimation of structural and dynamical properties of undercooled FeNi.

2. Simulation details

In this study, calculations have been performed using the Fe-Ni potential due to G. Bonny [8]. The potentials were fit to the following set of experimental data: elastic constants, vacancy formation energy and cohesive energy for Fe and Ni as well as the mixing enthalpy and defect properties for alloy compound FeNi and $FeNi_3$. The simulations were performed at zero external pressure to allow for a direct comparison to experiments under ambient pressure. Systems of N = 2048 atoms are put in a cubic simulation box with periodic boundary conditions. The number ratio of Fe and Ni is 1:1. MD simulations in the NPT ensemble were performed, and Newton's equations of motion are integrated with the velocity form of the Verlet algorithm using a time step of 1 fs. The masses of Ni and Fe atoms are set to m_{Ni} = 58.587 amu and m_{Fe} = 55.678 amu. First, the system is fully equilibrated at 1823 K by performing runs, i.e. 2×10^5 time steps in NPT systems. To keep the temperature constant, we apply the Andersen thermostat where after every 100 cycles we have chosen new velocities from a Maxwell–Boltzmann distribution in accordance with the temperature of the system. Next the average volume obtained from the simulation is used as an input for the following NVT ensemble. A further thermalisation is done in the NVT ensemble for 5×10^4 time steps. Finally, these equilibrated configurations are used as initial configurations for the production runs of the MD simulation in the NVE ensemble for another 2×10^5 time steps.

For the calculation of the structural, thermodynamical and dynamical properties in the undercooled state, appropriate care was taken to equilibrate the system at each new temperature: before starting the production runs at each lower temperature, an estimate of the equilibrium time was made by reasonable extrapolation of the relational time from higher temperature. In addition to the NPT runs, a further thermalisation was done in the NVT ensemble for the times larger than the estimated time in the MD simulation. These equilibrated configurations are used as initial configurations for the production runs of

MD simulations in the microcanonical ensemble. The temperatures considered are 3000 K, 2500 K, 2330 K, 2100 K, 1913 K, 1823 K, 1620 K, 1405 K, 1300 K, 1180 K and 1165 K. At the temperature of 1150 K, after 1×10^8 time step relaxation, corresponding to 100 ns real time, the system becomes crystal. While it is still in the undercooled liquid state at the temperature of 1165 K even the length of the equilibration and the production runs extended to 100 ns. To improve the statistics, five runs over independent initial configurations are performed at each temperature.

3. Results and discussion

3.1. *Liquid structure of undercooled FeNi*

3.1.1. *Partial pair correlation function (PPCF)*

A useful quantity to characterise the short-range order in a liquid is the pair correlation function. For a binary AB mixture, three partial PCFs are determined as

$$g_{\alpha\beta}(r) = \frac{N}{\rho N_\alpha (N_\beta - \delta_{\alpha\beta})} \left\langle \sum_{i=1}^{N_\alpha} \sum_{j=1}^{N_\beta} \delta(r - r_{ij}) \right\rangle \tag{1}$$

where the prime in the second sum means that i ≠ j if α = β, $_{\delta\alpha\beta}$ the Kronecker delta. Physically, $g_{\alpha\beta}(r)$ is propertional to the conditional probability of finding a particle of species β at a distance r from a particle of species α fixed at the centre. In case of an ideal gas, there are no correlations between the particles for all distance r. Then, the functions $g_{\alpha\beta}(r)$ are equal to one. For a liquid, the limit $g_{\alpha\beta}(r) \to 1$ is approached for $r \to \infty$. The partial static structure factor is $S_{\alpha\beta}(q)$ is defined by

$$S_{\alpha\beta}(q) = \frac{1}{N} \sum_{k_{\alpha=1}}^{N_\alpha} \sum_{l_{\beta=1}}^{N_\beta} \left\langle \exp\left\{ iq.\left[r_{k_\alpha} - r_{l_\beta} \right] \right\} \right\rangle \tag{2}$$

where the indices k_α, l_β correspond to the particles of species α and β, respectively (α, β = Ni, Fe). Due to the isotropy of the considered systems, structure factors depend on wave vector q only through the magnitude $q = |q|$. For all but the simplest model potentials, the functions $S_{\alpha\beta}(q)$ have to be determined from computer simulation or from scattering experiments, although disentangling the partial contributions in mixtures can be challenging for the latter.

We depict functions $g_{\alpha\beta}(r)$ for the different correlations at various temperatures in the range of 3000 K ≥ T ≥ 1165 K in Figure 1. For clarity of presentation, the curves are shifted from each other by a fixed distance on the ordinate. For Ni-Ni correlation, there is an increase in the height of the first peak with decreasing temperature, located around 2.42 Å, and at the lowest temperature, T = 1165 K. A splitting of the second peak into two peaks is seen with the position of first peak towards a larger r around 2.45 Å. The function of $g_{\mathrm{NiFe}}(r)$ and $g_{\mathrm{FeFe}}(r)$ shows similar behaviour, except that the amplitude of first peak of Fe-Fe is slightly lower than that of the Fe-Ni and Ni-Ni correlation. Here, the first peak of Fe-Fe correlation is located at 2.44 Å and 2.49 Å at the lowest temperature. The first peak of Fe-Ni correlation is almost the same as that of the Ni-Ni correlation, and it can be deduced that no stronger interaction of heterogenic atom pairs than those of the same atom pairs happens in FeNi melts, compared to other kinds of

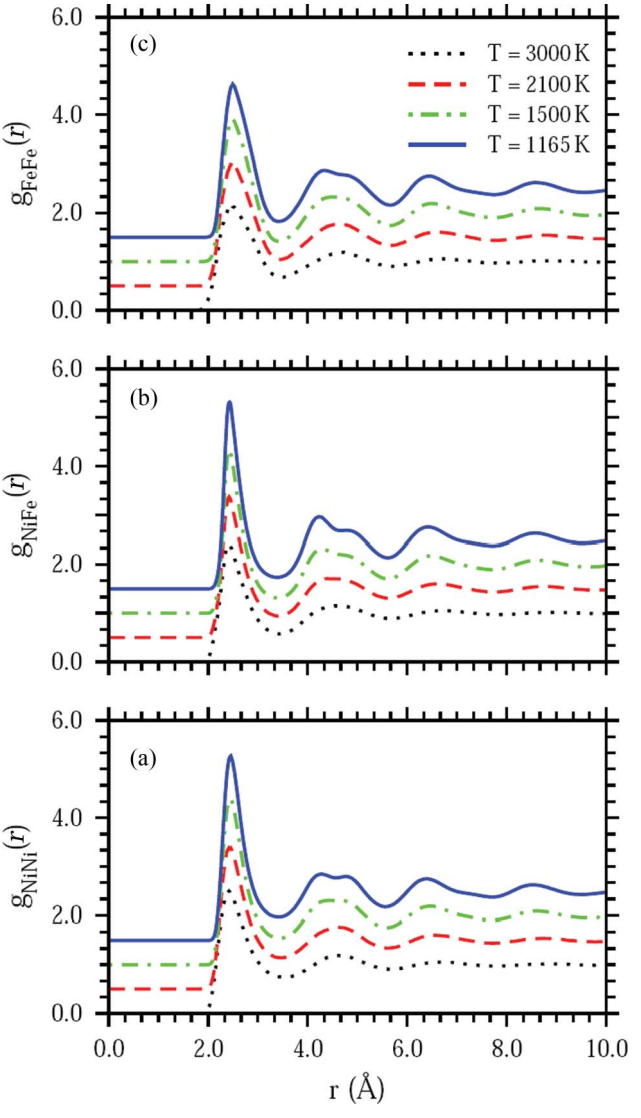

Figure 1. Partial PCF $g_{\alpha\beta}(r)$, (α, β = Ni, Fe) for (a) NiNi, (b) NiFe, (c) FeFe, at different temperatures, as indicated. For clarity of presentation, the curves at different temperatures are separated from each other in steps for 1.

binary liquids, for example, Ni20Al80 melts, where the first peak of Ni-Al shows the maximum among three PPCFs [9]. The interaction between Fe and Ni is quite similar to those of Ni-Ni and Fe-Fe. Further local structure analyses will be found in the distribution of coordination number.

3.1.2. *Coordination number distribution (CND)*

The coordination number (CN) of a liquid is defined as the average number of nearest neighbours about a given atom. The positions of neighbours are only statistically

describable. Based on the PCF, the coordination number of a liquid metal $N\alpha\beta(r)$ represents the number of type α particles around a type β particle plus the number of type β atoms around a type β atom at a distance r. The average coordination number is expressed as

$$\langle N_{\alpha\beta}(r)\rangle = \rho_{\alpha\beta}\int_0^r g(r)4\pi r^2 dr \tag{3}$$

In practice, the average coordination number, $\langle N(\mathrm{R})\rangle$ at a given R is obtained by counting

$$\langle N_{\alpha\beta}(R)\rangle = (N_\alpha(r \le R) + N_\beta(r \le R)) \tag{4}$$

Where $N_\alpha(r \le R)$ and $N_\beta(r \le R)$ are the number of type α particle (the coordination of a type β particle) and of type β particle (the coordination number of a type α particle). Individually, this constitutes the α – β pairs whose separations are less than or equal to R. We define the radius of the first – nearest – neighbour shell via the first minima of the PCF $g_{\alpha\beta}(r)$ It is useful to look at their distributions for a given radial distance r. The coordination distribution function $P(\mathrm{z})$ is represented as $N(r)$ as the function of particles. Usually, the physical scene of short-range order can be observed from the measured curves of the PCF from which the coordination number may be obtained. So far a number of experimental data concerned with the coordination numbers of liquid metals near the melting point have been reported due to the importance of understanding the local structure of liquid metals. The $P_{\alpha\beta}(z)$, shown in Figure 2, is symmetric for both NiNi, FeFe and FeNi. As we can infer from $P_{\mathrm{NiNi}}(z)$, the most likely values for the number of Ni neighbours around Ni atoms increases from 6–7 at a high temperature and up to 7–8 at a lower temperature; the number of Fe neighbours around Ni atom are $z = 5$ and $z = 6$ at low temperature. The $P_{\mathrm{NiFe}}(z)$ is unchanged even when the temperature decreases from 1500 K to 1165 K. A similar tendency can be observed in P_{FeFe}. Here, the most possible values for the number of Fe neighbours around the Fe atom are $z = 7$ and $z = 8$; in agreement with the behaviour observed for $g_{\alpha\beta}(r)$, Ni atoms seem to accept the Ni atom and Fe atom as its neighbours equally. This confirms that the FeNi melt is close to an ideal mixing system. The total numbers around Ni neighbours inferred from $P_{\alpha\beta}(\mathrm{z})$ in Figure 2 is between 11 and 13, and the coordination number we calculated is 12.6 at the temperature of 1165 K, which might suggest icosahedron short-range ordering (ISRO) in the undercooled liquid. As ISRO has already been observed from stable melts above the melting point both experimentally [10,11] and theoretically [12,13], it becomes more pronounced if the liquids are undercooled below the melting point.

3.1.3. *Partial structure factor of undercooled liquid FeNi*

For further analysis of the topological short-range order of liquid FeNi, the static Faber-Ziman (F-Z) structure factors $S_{\mathrm{NiNi}}(q)$, $S_{\mathrm{NiFe}}(q)$ and $S_{\mathrm{FeFe}}(q)$ describing the contributions to $S(q)$ are plotted in Figure 3. Obviously, no prepeak can be found in all three partial F–Z structure factors, indicating the absence of chemical short-range order (CSRO) in the liquid [9]. As CSRO is pronounced in the system where the heterogeneous atom pairs

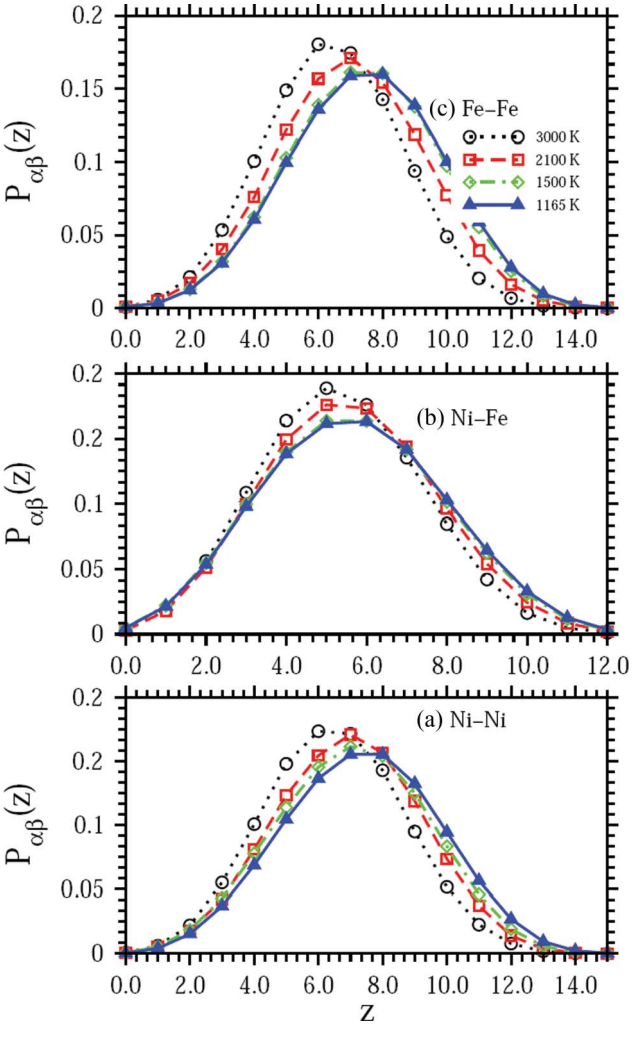

Figure 2. Coordination number distributions $P_{\alpha\beta}(z)$ for (a) β =NiNi, (b) αβ = NiFe, (c) αβ = FeFe at different temperatures.

have stronger interaction than that of homogeneous atom pairs, resulting in the preference of one kind of atom for having heterogeneous atom as nearest neighbours and being well separated from other homogeneous atoms, the avoidance of neighbouring homogeneous atom pairs leads to structural order on intermediated length scales, indicated by a pre-peak in one of F–Z structure factors. The second peaks of all partial structure factors split into two sub-peaks at lower temperature. A shoulder on the high-q side of the second peak of $S(q)$ has been taken as an indication of ISRO [14]. Furthermore, if the SRO is truly icosahedron, the relative positions of the different peaks in $S(q)$ are also expected to bear a distinct relationship with $q_{2nd}/q_{1st} \approx 1.71$ and $q_{shoulder}/q_{1st} \approx 2.04$ [15]. The calculated q_{2nd}/q_{1st} for $S_{NiNi}(q)$, $S_{NiFe}(q)$ and S_{FeFe} are 1.71, 1.71 and 1.69; corresponding $q_{shoulder}/q_{1st}$ is 1.97, 1.93 and 1.95 for the three species. Based on the peak shapes and similar ratio for peak position, combined with the calculated total coordinate number of

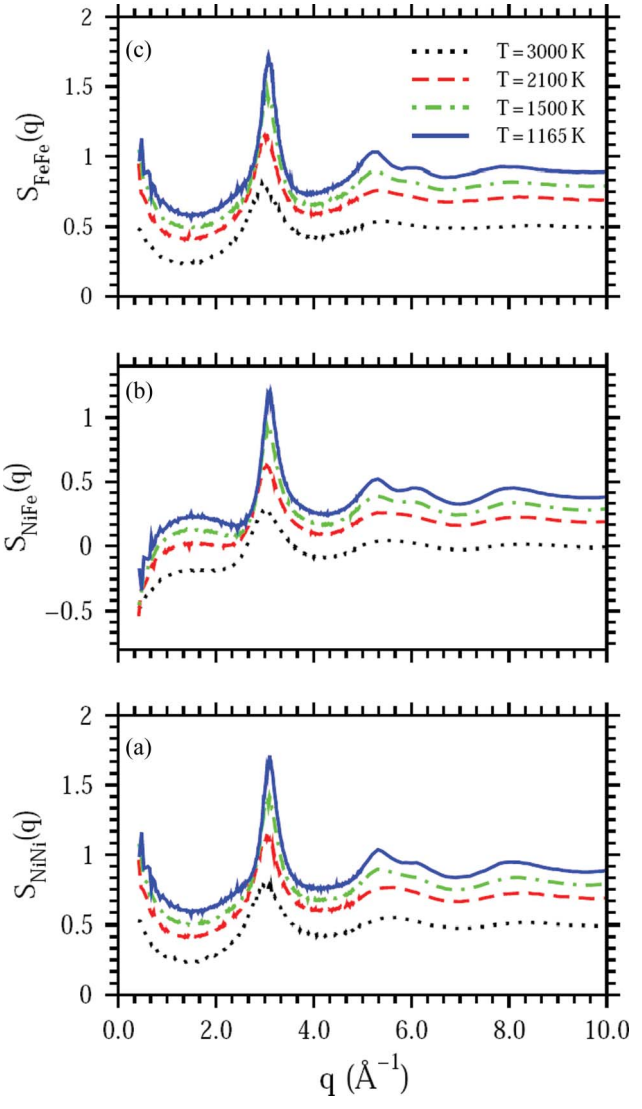

Figure 3. Partial structure factor $S_{\alpha\beta}(q)$ ($\alpha\beta$ = Ni, Fe) for (a) NiNi, (b) NiFe, (c) FeFe, at different temperatures, as indicated. For clarity of presentation, the curves at different temperatures are separated from each other in steps for 0.2.

the liquid, it is inferred that the topological SRO in FeNi melt corresponds to icosahedron. As long as the atomic radii of the alloy components are similar, it can be assumed that an ISRO will be advantageous [16], which seems to indicate an ISRO prevailing in FeNi melts since the R_{Ni}/R_{Fe} = 1.06, much less than 1.25, which is considered as the maximum ratio of atomic radii of the component alloys to be favourable for the ISRO in melts both experimentally [17,18] and theoretically [19]. Further structural analysis should be made to test if the icosahedra exist in FeNi melts.

Bonded pairs are the smallest structural unit in liquid metals. There are a large number of bonded pairs in the liquid metals accordingly manifesting the feature of short-range

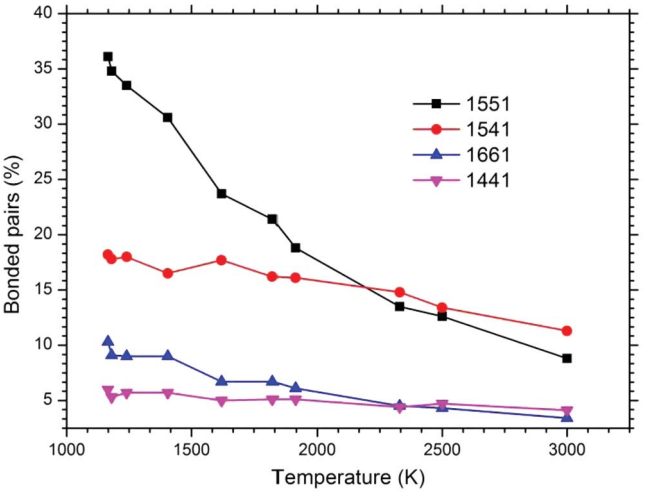

Figure 4. Bonded pairs as a function of temperature.

order of liquid metals. Figure 4 describes the changes of the bonded pairs with the temperature. The numbers of 1661 and 1441 bonded pairs representing bcc type structure are unchanged during the cooling process. The number of 1551 and 1541 bonded pairs corresponding to an icosahedron cluster increases rapidly as the temperature drops. The number of 1551 bonded pairs makes up 9% of all kinds of bonded pairs in the melts. With decreasing temperature, the number of 1551 bonded pairs increases to 36%, occupying a predominant position in the system, and the number of 1541 bonded pairs show the same tendency increasing from 11% to 18%. One icosahedron is made up of 12,1551 bonded pairs, which indicates the existence of icosahedra in the FeNi melt in the deep undercooled state. Figure 5 shows all icosahedron clusters found in undercooled FeNi at the temperature of 1165 K.

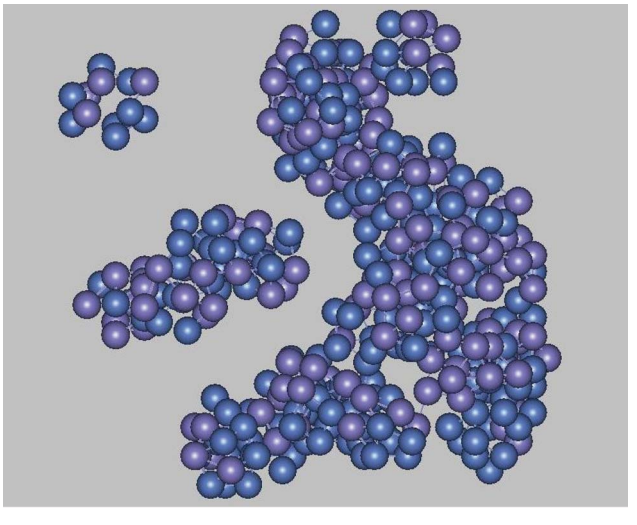

Figure 5. All icosahedra in FeNi melts at temperature of 1165 K, the blue one represents Fe atom and the pink one represents Ni atom.

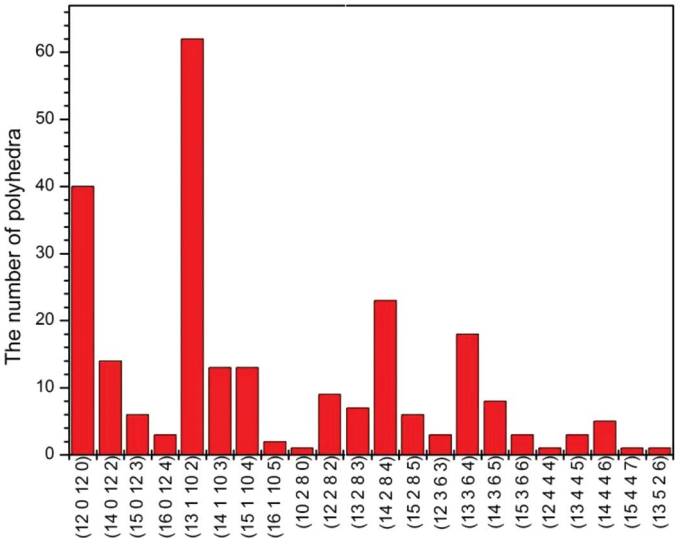

Figure 6. Polyhedra in undercooled FeNi melts at temperature of 1165 K.

The cluster-type index method (CTIM) is adopted to describe some of the important kinds of clusters, namely icosahedrons cluster, defect icosahedrons clusters, etc. by using four integers. The first index represents the number of surrounding atoms which along with a central atom form a cluster. The second, third and fourth integers represent the numbers of 1441, 1551 and 1661 bond types, respectively. According to the CTIM, we have obtained the statistic numbers of various types of clusters as shown in Figure 6. The number of (12 0 12 0) clusters representing icosahedrons is 40 in simulated 2048 atoms, a little lower than that of the (13 1 10 2) cluster, which is a typical defective icosahedron. Besides these clusters, many other kinds of clusters, for example, (14 0 12 2) cluster, (14 2 8 4) cluster and (13 3 6 4) cluster exist in the undercooled FeNi melts, which shows the diversity of the liquid structure.

3.2. *Dynamics of FeNi Melts*

3.2.1. *Mean-square-displacement (MSD)*

The time correlation functions are very useful in the theoretical and experimental study of dynamical and transport properties of liquids. Normally, the mean squared displacement (MSD) is used to characterise the relaxation dynamics of undercooled melts, defined as

$$\left\langle r_{\alpha}^{2}(t)\right\rangle = \left\langle \left[r_{t,\alpha}(0) - r_{t,\alpha}(t)\right]^{2}\right\rangle \tag{5}$$

where $r_{t,\alpha}$ denotes the position of a tagged particle of type α (α = Fe, Ni) at time t, and [...] implies the average over independent runs as well as over particles of the same species.

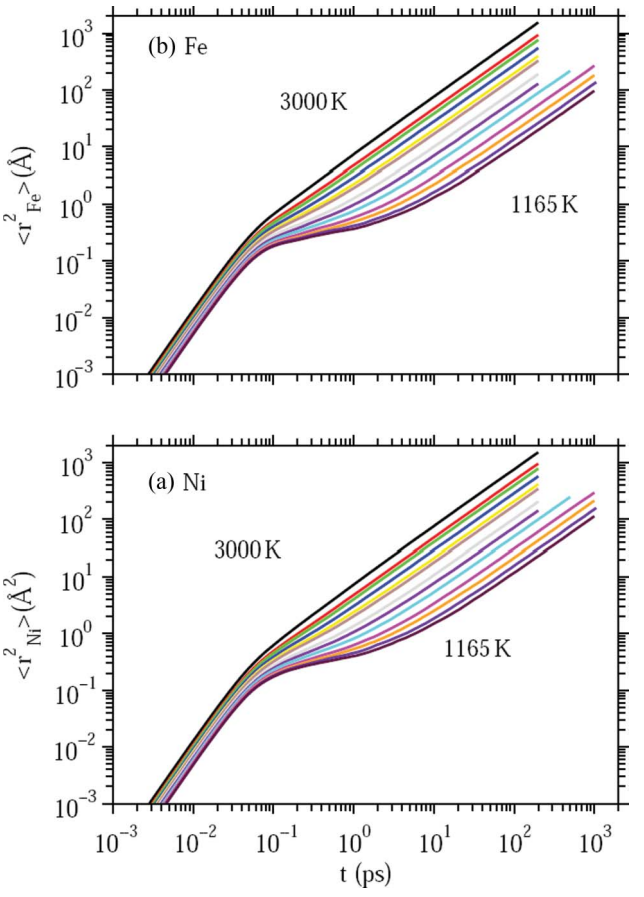

Figure 7. Double logarithmic plot of the mean-squared displacements as a function of time t for (a) Ni atoms and (b) Fe atoms. The results for all the simulated temperatures in the range from 1165 to 3000 K are shown.

The self-diffusion constant for a particle of species is α obtained by $\langle r_\alpha^2 \rangle = 6D_\alpha t$. In Figure 7, the MSD for Ni and Fe particles for all simulated temperatures are shown on a log-log scale, and they are almost identical at the given temperature. At a high temperature, a crossover from a ballistic regime ($\propto t^2$) at short time to a diffusive regime ($\propto t$) at long time can be seen. At a lower temperature, a plateau is observed at intermediate times, where MSD does not increase. This plateau caused by the long-range diffusion of atoms indicates the onset of the 'cage effect', as each atom sits in a 'cage' formed by its nearest neighbours, and the lower the temperature is, the more time it takes until the atom can 'escape from the cage'. Note that the MSD reaches 100 Å^2 on a time-scale of no more than 1 ns at the temperature of 1165 K, and further structural relaxation under a lower temperature will lead to the crystallisation of the undercooled liquid. In contrast to that of Ni20Al80 melts, its structural relaxation time reaches 100 ns [9] as the MSD reaches 100 Å^2, which means that the atom diffusion is limited in Ni20Al80, and it is more difficult for the particles to escape from the 'cage'. Ni20Al80 undercooled liquid can remain more stable in a wide temperature range without crystallisation. According to the energy landscape theory [20], longer dynamical relaxation time and a more stable structure in

the undercooled liquid means higher glass formation ability. For the FeNi melts, on the contrary, it shows weaker glass formation ability, compared to the Ni20Al80 melts.

3.2.2. *Diffusion coefficient of FeNi Melts*

The Ni, Fe self-diffusivity determined for FeNi melts as a function of temperature is plotted in Figure 8. The self-diffusion coefficient D_{Ni} and D_{Fe} from simulation are quite similar in the investigated temperature regimes. The D (T) of the liquid FeNi shows essentially an Arrhenious-type behaviour $D = D_0\exp(-E_A/k_BT)$ above the temperature of 1500 K with E_A(Ni) = 0.60 eV, D_0 = 1.24 × 10^{-7} m^2/s for Ni and E_A(Fe) = 0.62 eV, D_0 = 1.40 × 10^{-7} m^2/s for Fe. The self-diffusivity of Ni and Fe is quite similar, as we have shown with respect to the MSD, which indicates that Ni atoms are as localised as Fe atom. The experimental self-diffusion coefficient of liquid FeNi is not available in the literature. However, it is listed in other liquid binary alloys: the self-diffusion constant is $D_0 \approx 10^{-8}$ m^2/s from both experiment and simulation, and activation energy is E_A = 0.36 eV for Ni20Al80 melts in a recent publication [21]; the measured self-diffusion constant and activation energy of Ni in Ni36Zr64 melts are D_0 = 2.1 × 10^{-7} m^2/s and E_A = 0.64eV, respectively [22]. The diffusion constant and activation energy of Ni are quite similar between FeNi and Ni36Zr64 melts, while the structural relaxation shows significant difference: FeNi melt is close to an ideal mixing system, with no stronger interaction of Fe-Ni atom pairs than those of Fe-Fe or Ni-Ni atom pairs; the absence of pre-peak in F-Z structure factor suggests the avoidance of CSRO in the FeNi melt. However, the CSRO prevailed in both Ni36Zr64 and Ni20Al80 melts, which results in the speculations about a possible link between CSRO and glass-forming ability.

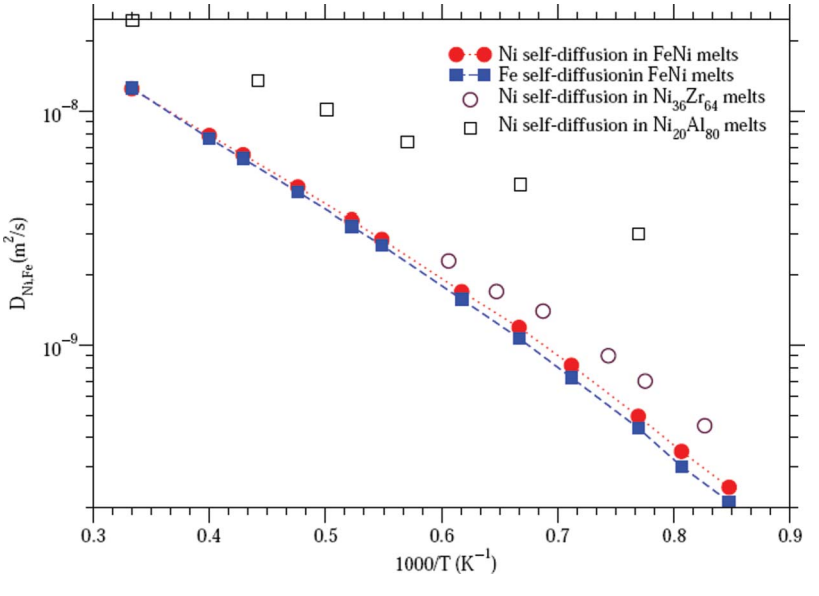

Figure 8. Diffusion coefficient as a function of temperature. The filled symbols represent present work; the open symbols are obtained from reference Ni self-diffusion for $Ni_{20}Al_{80}$ [21] and for Ni36Zr64 [23].

4. Conclusion

MD simulation has been performed to explore structural and dynamical properties in the undercooling condition based on EAM energetics and interatomic forces. FeNi shows a homogeneous structure, although the diffusion constant of Ni and the activation energy for FeNi melts are comparable to that of Ni36Zr64, which is proved to be a good glass former experimentally. In this work, we can conclude that an icosahedrons cluster exists in undercooled FeNi melts, and no CSRO is found in it. MSD curves indicate that FeNi has shorter dynamical relaxation time in the undercooled liquid.

Acknowledgement

I thank National Science Foundation of Shandong Province (ZR2010EM030) and National Science Foundation of China (No. 51171091) for financial support.

Reference

[1] Y. Waseda, H.S. Chen, K.T. Jacob, and H. Shibata, Sci. Technol. Adv. Mater. **9**, 023003 (2008).
[2] A. Inoue, Acta Materialia. **48**, 279 (2000).
[3] D.B. Miracle, Nature Mater. **3**, 697 (2004).
[4] F.C. Frank, Proceedings of the Royal Society of London. Series A, Math. Phys. **215**, 43 (1952).
[5] V. Wessels, A.K. Gangopadhyay, K.K. Sahu, R.W. Hyers, S.M. Canepari, J.R. Rogers, M.J. Kramer, A.I. Goldman, D. Robinson, J.W. Lee, J.R. Morris, and K.F. Kelton, Phys. Rev. B., **83**, 094116 (2011).
[6] W.H. Wang, C. Dong, and C.H. Shek, Mater. Sci. Eng. R. **44**, 45 (2004).
[7] C.A. Angell, Sci. **267**, 1924 (1995).
[8] G. Bonny, Modeling. Simul. Mater. Sci. Eng. **17**, 025010 (2009).
[9] S.K. Das, J. Horbach, and T. Voigtmann, Phys. Rev. B **78**, 064208 (2008).
[10] A.K. Gangopadhyay, K.F. Kelton, G.W. Lee, and R.W. Hyers, Phys. Rev. Lett. **90**, 195504 (2003).
[11] K.F. Kelton, G.W. Lee, A.K. Gangopadhyay, and R.W. Hyers, Phys. Rev. Lett. **93**, 037802 (2004).
[12] H. Jonsson and H.C. Andersen, Phys. Rev. Lett. **60**, 2295 (1988).
[13] D.R. Nelson and S. Sachdev, Phys. Rev. Lett. **53**, 1947 (1984).
[14] G.W. Lee, A.K. Gangopadhyay, R.W. Hyers, and T.J. Rathz, Phys. Rev. B **7**, 184102 (2008).
[15] S. Sachdev and D.R. Nelson, Phys. Rev. Lett. **53**, 1947 (1984).
[16] H. Jonsson and H.C. Andersen, Phys. Rev. Lett. **60**, 2295 (1988).
[17] T. Schenk, V. Simonet, D.H. Moritz, and R. Bellissent, Europhys. Lett. **65**, 34 (2004).
[18] V. Simoner, F. Hippert, M. Audier, and R. Bellssent, Phys. Rev. B **65**, 024203 (2001).
[19] M. Ronchetti and S. Cozzini, Mater. Sci. Eng. A **178**, 19 (1994).
[20] M. Shimono and H. Onodera. Mater. Trans. **45**, 1163–1171 (2004).
[21] J. Horbach, S.K. Das, and A. Griesche, Phys. Rev. B **75**, 174304 (2007).
[22] N.P. Bailey, J. Scjoptz, and K.W. Jacobsen, Phys. Rev. B **69**, 144205 (2004).
[23] D.H. Moritz, S. Stueber, and H. Hartmann, Phys. Rev. B **79**, 064204 (2009).